UNIVERSITÀ
DEGLI STUDI
DI PADOVA

Università degli Studi di Padova

Padua Research Archive - Institutional Repository

Phase-Sensitive Mode Conversion and Equalization in a Few Mode Fiber Through Parametric Interactions

Original Citation:

Availability:
This version is available at: 11577/3227551 since: 2017-05-10T16:53:07Z

Publisher:
Institute of Electrical and Electronics Engineers Inc.

Published version:
DOI: 10.1109/JPHOT.2016.2644958

Terms of use:
Open Access

This article is made available under terms and conditions applicable to Open Access Guidelines, as described at http://www.unipd.it/download/file/fid/55401 (Italian only)

(Article begins on next page)

IEEE Photonics Journal
An IEEE Photonics Society Publication

Open Access

Phase-Sensitive Mode Conversion and Equalization in a Few Mode Fiber Through Parametric Interactions

Volume 9, Number 1, February 2017

Abderrahmen Trichili
Mourad Zghal
Luca Palmieri
Marco Santagiustina

IEEE Proof

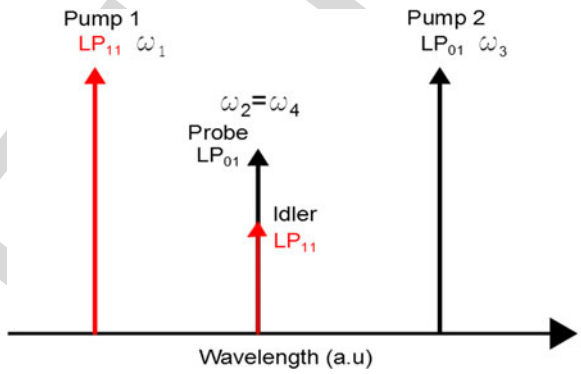

DOI: 10.1109/JPHOT.2016.2644958
1943-0655 © 2016 IEEE

IEEE photonics SOCIETY

IEEE

Phase-Sensitive Mode Conversion and Equalization in a Few Mode Fiber Through Parametric Interactions

Abderrahmen Trichili,[1,2] Mourad Zghal,[1,3] Luca Palmieri,[2] and Marco Santagiustina[2]

[1]GreS'Com Laboratory, Engineering School of Communication of Tunis (Sup'Com), University of Carthage, Ariana 2083, Tunisia
[2]Dipartimento di Ingegneria dell'Informazione, Università di Padova, Padova 35131, Italy
[3]Institut Mines-Télécom/Télécom SudParis, Evry 91011, France

DOI:10.1109/JPHOT.2016.2644958
1943-0655 © 2016 IEEE. Translations and content mining are permitted for academic research only. Personal use is also permitted, but republication/redistribution requires IEEE permission. See http://www.ieee.org/publications_standards/publications/rights/index.html for more information.

Manuscript received October 15, 2016; revised December 14, 2016; accepted December 16, 2016. This work was supported by the International Centre for Theoretical Physics ICTP affiliated center "the Optical Society of Tunisia." The work of A. Trichili was supported in part by the University of Carthage and in part by the Dipartimento di Ingegneria dell'Informazione, Università di Padova, under Project Photon1. Corresponding author: M. Santagiustina (e-mail: marco.santagiustina@unipd.it).

Abstract: The parametric interaction in few mode fibers is theoretically and numerically studied in the particular case in which the signal and the idler waves are frequency degenerate but mode nondegenerate. Under simplifying hypotheses, we derive analytical formulas for the phase-insensitive and phase-sensitive amplification gain and conversion efficiency. The analytical formulas are in very good agreement with the numerical solutions of a full vectorial model that takes into account losses, mode coupling, and all possible four-wave mixing interactions. In the phase-sensitive regime, we predict that for small input pump powers, a large and tunable phase-sensitive extinction ratio can be achieved on one mode, whereas the other mode power remains essentially unaffected. Finally, in the high-gain regime, the self-equalization of the output power on different modes can be also achieved.

Index Terms: Nonlinear optical devices, fiber nonlinear optics, optical fiber devices.

1. Introduction

Spatial division multiplexing (SDM) is the ultimate multiplexing technique and is now widely studied to overcome the incoming "capacity crunch" [1], [2] by exploiting several spatial modes to transmit information [3]. A considerable research work has been recently devoted to clarify the impact of the fiber nonlinearities on SDM [4]–[7]. Among nonlinear effects, four wave mixing (FWM) in multimode fibers has been demonstrated long ago [8]. Seminal theoretical studies of degenerate FWM in short photonic crystal fibers showed that FWM is responsible for energy transfer between modes [9]–[11]. For longer few mode fibers (FMFs), various intermodal (IM) non-degenerate FWM processes have been investigated [12], [13], and the potential of IM-FWM for broadband wavelength conversion close to the zero dispersion wavelength (1.3 μm) has been highlighted [14]. However, several features of IM-FWM in FMFs are still largely unexplored. In particular, it is well known that FWM enables both phase-insensitive and phase-sensitive amplification (PIA, PSA) [15], [16], the latter effect showing a high potential in extending the reach of the fiber optics links, owing to the fact that noise figure can decrease below the 3 dB quantum limit of PIA [17]. In the context of multimode

IEEE PROOF

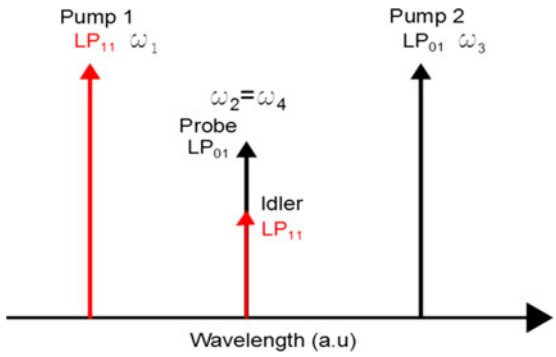

Fig. 1. IM-FWM process considered here entails an idler wave at the same frequency of the probe signal but propagating on a different spatial mode. The pumps are also launched in two different spatial modes.

waveguides PSA was studied but only in $\chi^{(2)}$ nonlinear media [18]. The aim of this paper is to extend the knowledge and to hint at the exploitation of FWM for realizing useful FMF devices. With this objective in mind we consider a particular case of the IM-FWM occurring in a FMF where the mode families LP_{01} and LP_{11} can propagate, that is when the signal and the idler waves are mode non-degenerate but are frequency degenerate. This condition actually implies that FWM processing functions can be realized at the same frequency but on different fiber modes. We will first show that, in the undepleted pump approximation and neglecting mode coupling, approximate expressions for the PIA and PSA gain can be derived, in spite of the fact that the nonlinear coefficients are different because waves propagate on different modes. The predictions of the derived analytical formulas are in excellent agreement with the numerical simulations of a model considering all FWM interactions, pump depletion, losses and low mode coupling and so are a valuable tool to study IM-FWM. The present work is aimed at highlighting features of the PSA regime that could be exploited to realize mode processing devices. For example we will show the existence of an extremely large phase-sensitive mode extinction ratio at low input pump powers and the self-equalization of the mode power content at the IM-FWM amplifier output. The paper is organized as follows. In Section II, we will explain why the selected IM-FWM process can be reasonably considered the only significant FWM process occurring in the fiber, so justifying a model reduced to four waves. In Section III, we will derive analytical formulas of gain and conversion efficiency, while in Section IV, the full vectorial model used for numerical integrations will be briefly presented. Finally, in Section V, we will present the comparison of the theoretical and numerical results and highlight FWM mode processing.

2. Theoretical Approach

In FWM, two pumps at frequencies ω_1 and ω_3 co-propagating inside a fiber interact with a probe signal at frequency ω_2 and an idler wave at frequency ω_4 satisfying the photon energy conservation relation $\omega_4 = \omega_1 - \omega_2 + \omega_3$. When a probe and an idler are launched at different frequencies or in different modes, the FWM is non-degenerate. Here, we are interested in the non-degenerate IM-FWM depicted in Fig. 1, in which the probe signal and the idler are propagating on different modes of a FMF, but $\omega_2 = \omega_4$. This is a special case of the interaction denoted as PROC1 in [12] and [13], but it was not considered in those papers. It also bears similarity to the vector FWM process studied in [19]. The efficiency of the FWM interaction depends on the linear phase mismatch parameter

$$\Delta\beta = \beta^{(m)}(\omega_2) + \beta^{(n)}(\omega_4) - \beta^{(o)}(\omega_1) - \beta^{(p)}(\omega_3), \tag{1}$$

where $\beta^{(l)}(\omega_h)$ is the propagation constant of the wave at frequency ω_h propagating in the l^{th} fiber mode, that can be approximated by a Taylor expansion around an arbitrary frequency ω_0

$$\beta^{(l)}(\omega_h) \approx \beta_0^{(l)} + \beta_1^{(l)}\Delta\omega_h + \frac{1}{2}\beta_2^{(l)}\Delta\omega_h^2 + \frac{1}{6}\beta_3^{(l)}\Delta\omega_h^3. \tag{2}$$

IEEE Proof

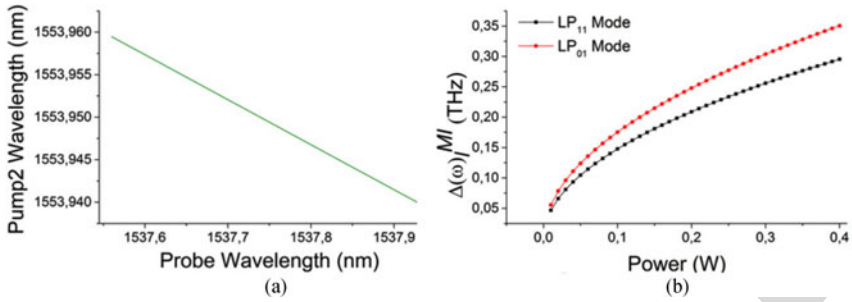

Fig. 2. (a) Pump 2 wavelength satisfying the linear phase matching condition as a function of the probe signal (and idler) wavelength $\lambda_{2,4}$ (pump 1 wavelength is fixed at $\lambda_1 = 1521.885$ nm). (b) Modulation instability gain band as a function of the input pump power for each mode of the FMF.

The dispersion coefficients $\beta_k^{(l)} = \partial^k \beta^{(l)} / \partial \omega^k$ ($k = 0, 1, 2, 3$) are calculated at ω_0 and $\Delta\omega_h = \omega_0 - \omega_h$. Here, for the sake of simplicity, we will consider fiber parameters defined like those of [12], [13] at the central wavelength $\lambda_0 = 2\pi c_0/\omega_0 = 1540$ nm: $\beta_2^{\mathrm{LP}_{01}} = -24.3$ ps^2/km , $\beta_2^{\mathrm{LP}_{11}} = -23.04$ ps^2/km; $\beta_1^{\mathrm{LP}_{01}} - \beta_1^{\mathrm{LP}_{11}} = -300$ ps/km. Moreover, the fiber length is $L = 4.7$ km and the loss coefficient is $\alpha = 0.226$ dB/km for all modes. In FMFs the nonlinear coefficients depend on the modes involved in IM-FWM [9], [13]: if modes $\{m, n, o, p\}$ (as labelled in Eq. 1) are involved, the nonlinear coefficient is given by $\gamma\, f_{mnop}$, where $\gamma = 1.77$ W^{-1}km^{-1} and f_{mnop} is the normalized mode overlap integral, whose definition can be found in [13, eq. 11], and is not reported here for the sake of brevity. For this fiber we fixed the wavelength λ_1 of pump 1 at 1521.885 nm and numerically determine the wavelengths of the other pump and of the signal/idler satisfying the photon energy conservation and $\Delta\beta = 0$; the result is shown in Fig. 2(a).

Similarly to what shown in [8], [12], [13], also in the present case the phase matching condition is very narrow band (its FWHM is estimated to be about 0.2 nm) and this actually enables to neglect other processes (i.e. PROC 2 and PROC3 as defined in [12], [13]). As pointed out in [14] modulation instability (MI) of the pumps, stimulated by waves co-propagating in the same mode might also occur. For the situation described in Fig. 1 and for the FMF under examination, the half-width of the MI band on mode l can be estimated as [20]

$$\Delta\omega_l^{MI} < \sqrt{\frac{4 f_{llll} \gamma \mathrm{P}_l}{|\beta_2^{(l)}|}} \tag{3}$$

where P_l is the input pump power on mode l. Setting $\lambda_1 = 1521.885$ nm, $\lambda_3 = 1553.95$ nm and $\lambda_2 = \lambda_4 = 1537.75$ nm, the detuning $\omega_2 - \omega_1 = \omega_3 - \omega_4 \simeq 12.7$ THz is much larger than $\Delta\omega_l^{MI}$ calculated from (3) as presented in Fig. 2(b). Therefore, the pump-signal and the pump-idler MI can be reasonably neglected.

3. Analytical Formulation

According to the above argumentation, the coupled equations describing the process of Fig. 1 for continuous waves (CWs) are

$$\frac{dA_{P1}}{dz} = i\gamma[f_{1111}|A_{P1}|^2 A_{P1} + 2(f_{1122}|A_S|^2 + f_{1133}|A_{P2}|^2 + f_{1144}|A_I|^2)A_{P1} + 2f_{1234} A_S A_I A_{P2}^* \exp(i\Delta\beta z)] \tag{4}$$

$$\frac{dA_S}{dz} = i\gamma[f_{2222}|A_S|^2 A_S + 2(f_{2211}|A_{P1}|^2 + f_{2233}|A_{P2}|^2 + f_{2244}|A_I|^2)A_S + 2f_{2134} A_{P1} A_{P2} A_I^* \exp(-i\Delta\beta z)] \tag{5}$$

$$\frac{dA_{P2}}{dz} = i\gamma[f_{3333}|A_{P2}|^2 A_{P2} + 2(f_{3311}|A_{P1}|^2 + f_{3322}|A_S|^2 + f_{3344}|A_I|^2)A_{P2} + 2f_{3241} A_S A_I A_{P1}^* \exp(i\Delta\beta z)] \tag{6}$$

IEEE Proof

$$\frac{dA_I}{dz} = i\gamma[f_{4444}|A_I|^2 A_I + 2(f_{4411}|A_{P1}|^2 + f_{4422}|A_S|^2 + f_{4433}|A_{P2}|^2)A_I + 2f_{4132}A_{P1}A_{P2}A_S^* \exp(-i\Delta\beta z)] \quad (7)$$

where A_{P1}, A_{P2}, A_S, and A_I are the slowly varying complex envelopes of pump 1, pump 2, signal and idler, respectively (for the sake of simplicity in (4)–(7) the modal dependence of the normalized overlap integrals f_{mnop} is indicated by the respective frequency index). On the right hand side of each equation, the first term represents self-phase modulation (SPM), the summation cross-phase modulation (XPM) and the last term the non-degenerate IM-FWM. As previously mentioned, the nonlinear coefficient of each term depends on a different overlap integral f_{mnop}. Therefore, (4)–(7) mathematically resemble those of nonlinearly dispersive waveguides [21], [22] and exact expressions of gain and conversion efficiency can be found in the undepleted pump approximation defined in [23, Sec. 2.6]. First, the pump equations are solved to yield $A_{P1}(z) = \sqrt{P_{P1}}\exp[i\gamma(f_{1111}P_{P1} + 2f_{1133}P_{P2})z + i\phi_{P1}]$, $A_{P2}(z) = \sqrt{P_{P2}}\exp[i\gamma(f_{3333}P_{P2} + 2f_{3311}P_{P1})z + i\phi_{P2}]$, where $\phi_{P1,P2}$ are the pump input phases and introducing the following change of variables:

$$B_S(z) = A_S \exp[-2i\gamma((f_{2211}P_{P1} + f_{2233}P_{P2})z] \quad (8)$$

$$B_I(z) = A_I \exp[-2i\gamma((f_{4411}P_{P1} + f_{4433}P_{P2})z] \quad (9)$$

the governing equations for the signal and the idler simplify into

$$\frac{dB_S}{dz} = i\gamma r B_I^* \exp[(i\phi_{P1} + \phi_{P2})]\exp(-i\Phi z), \quad \frac{dB_I^*}{dz} = -i\gamma r B_S \exp[-(i\phi_{P1} + \phi_{P2})]\exp(i\Phi z) \quad (10)$$

where

$$\Phi = \gamma q + \Delta\beta \quad (11)$$

is the nonlinear phase mismatch, and

$$r = 2\sqrt{P_{P1}P_{P2}}f_{4132}, \quad q = f_{4411}P_{P1} + f_{2233}P_{P2}. \quad (12)$$

The conditions $f_{4132} = f_{2134}$, $f_{2233} = f_{3333}$, $f_{4411} = f_{1111}$, $f_{2211} = f_{1133} = f_{4433}$ that derive from the mode selection rules [13], [24] have been applied to calculate (10). Note that, like in [21], the nonlinear effective coefficients defining the maximum gain (γr) and the nonlinear contribution to the phase matching (γq) in (12) are different (in SMFs they are equal). Equation (10) can be solved by following the guideline of [23, Sec. 2.6]. Note that so far losses have been neglected; exact formulas for the mode gain and the mode conversion efficiency might be determined also with mode dependent losses, similarly to what found in [25]. That formulation involves special functions and does not enable to quickly grasp the interesting features of the IM-FWM. However, if total losses are small and are not mode dependent, pump losses can be accounted for by substituting the fiber length L with the effective length $L_{eff} = (1 - \exp(\alpha L))/\alpha$, while signal and idler losses can be simply accounted for by multiplying lossless gain and conversion efficiency expressions by $\exp(-\alpha L)$. We will demonstrate (Section V) that the results of this approximation are in excellent agreement with the numerical results of the full model that includes losses (see Section IV). If we assume that $A_I(z = 0) = 0$, we can prove that the PIA gain for the signal is found:

$$G_S^{PIA} = \frac{P_S(L)}{P_S(0)} = \left[1 + \left(1 + \frac{\Phi^2}{4g^2}\right)\sinh^2(gL_{eff})\right]\exp(-\alpha L). \quad (13)$$

where

$$g = \sqrt{(\gamma r)^2 - \left(\frac{\Phi}{2}\right)^2}. \quad (14)$$

We can similarly determine the idler conversion efficiency:

$$\eta_I^{PIA} = \frac{P_I(L)}{P_S(0)} = \left[\left(1 + \frac{\Phi^2}{4g^2}\right)\sinh^2(gL_{eff})\right]\exp(-\alpha L). \quad (15)$$

IEEE Proof

Note that $G_S^{PIA} = \eta_I^{PIA} + \exp(-\alpha L)$ as expected from the conservation of the number of photons (the so called Manley-Rowe relations detailed in [23, Sec. 2.5]) and because signal and idler are frequency degenerate. Let us stress, however, that the idler is generated on a different mode with respect to the signal, and therefore, (15) actually defines the efficiency of a mode converter at the same frequency based on FWM.

The PSA regime is found when $A_I(z=0) \neq 0$ [15] and, to the best of our knowledge, it has not been explored in the context of FMFs. In this regime the signal and idler amplification gains can be written as

$$G_{S,I}^{PSA} = G_S^{PIA} + \Delta G_{S,I}, \tag{16}$$

where the phase-sensitive excess gains (or attenuation) can be proved to read

$$\Delta G_{S,I} = \left(\frac{\gamma r U_{S,I}}{g}\right)^2 \sinh^2(gL_{eff}) \left[1 + \frac{2g}{\gamma r U_{S,I}} \cos(\phi_T) \coth(gL_{eff}) - \frac{\Phi}{\gamma r U_{S,I}} \sin(\phi_T)\right] \exp(-\alpha L) \tag{17}$$

where $U_S = R, U_I = 1/R$, $\phi_T = \phi_S + \phi_I - \phi_{P1} - \phi_{P2} - \pi/2$ (ϕ_S and ϕ_I are the signal and idler phases) and $R = |A_I^*(0)/A_S(0)|$ is the amplitude ratio between signal and idler waves at the fiber input. Note that, for $R = 1$, $\Delta G_S = \Delta G_I$. From (16) and (17), another important figure of merit characterizing PSA, i.e., the phase-sensitive extinction ratio (PER), can be also calculated:

$$PER_{S,I} = 10\log_{10}\left[\frac{\max_{\phi_T}\{G_{S,I}^{PSA}\}}{\min_{\phi_T}\{G_{S,I}^{PSA}\}}\right] = 10\log_{10}\left[\frac{G_{S,I}^{MAX}}{G_{S,I}^{min}}\right]. \tag{18}$$

The PER quantifies the dynamic range of the PSA amplitude squeezing between in-phase and in-quadrature components [26]. Its maximization is highly searched for PSA applications like low noise amplification, phase- and amplitude- regeneration [26]–[28]. In this paper it actually quantifies the range over which the PSA can vary the power distribution on the different modes of the FMF.

4. Full Model of FWM

The analytical results reported above must be compared with solutions when all simplifying hypotheses are removed, i.e. with all nonlinear mixing terms, depleted pumps, losses and mode coupling. To this aim we consider a system of 18 equations that accounts for all FWM processes [14] that could mix three different frequencies (ω_1, $\omega_2 = \omega_4$ and ω_3) each with components on the two polarization modes of the three spatial modes (the LP_{01} and the two degenerate modes LP_{11a} and LP_{11b}). In each equation a term accounting for equal losses has been introduced. In FMFs random linear mode coupling, can be induced by various physical effects such as bending, tension, twisting, rotation, pressure and imperfections in the fiber core shape and refractive index [29], and it is strongly dependent on the the difference of propagation constants of the modes [30]. Though for the fiber defined in [13] (whose parameters are also used here) coupling effects were negligible for reasonable strengths of coupling mechanisms we preferred, for the sake of precision, to account for some coupling (birefringence and core ellipticity) by adopting a model, whose details can be found in [31]. The key element of the model is the angle θ describing the orientation of the perturbation changing randomly with z according to the Wiener process [32] $d\theta/dz = -\sigma\eta(z)$, where $\eta(z)$, is a zero mean, Gaussian white noise with autocorrelation $r_\eta(z) = \delta(z)$, and $\sigma = 1/L_F$ is the inverse of the correlation length L_F. In our study, we tested a few values of the correlation length ($L_F = 10, 100, 1000$) m, and we present the results for $L_F = 10$m that implies a very perturbed fiber, i.e. the worst case. Two values of the birefringence $\Delta n = 10^{-6}, 10^{-5}$ were also tested and we present the results for $\Delta n = 10^{-6}$ that is a more typical value. For core ellipticity, we assume that the maximum ratio between maximum core radius variation and the core radius is $r_e = 10^{-3}$. As expected for such short fiber random mode coupling introduces negligible changes for all the used values of the parameters, similarly to what is shown in [13].

IEEE Proof

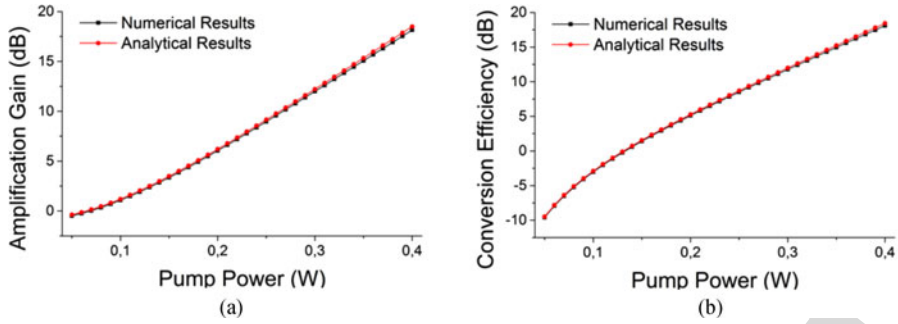

Fig. 3. (a) Gain and (b) mode conversion efficiency, at perfect matching, as functions of the input pump powers $P_{P1} = P_{P2}$. The input signal power was $P_S = 0.1$ mW. Red curves are the analytical results [see 13 and 15], while black curves the numerical ones.

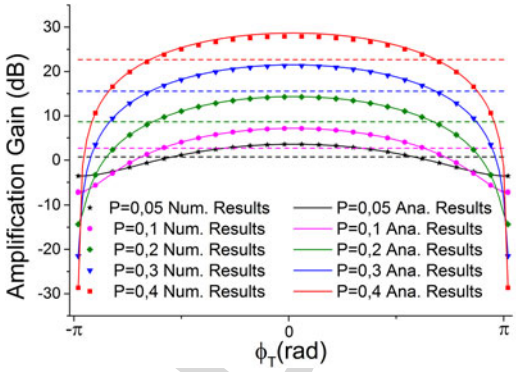

Fig. 4. PSA gain as a function of the phase ϕ_T for various values of the input pump powers (0.4, 0.3, 0.2, 0.01, and 0.05 W, respectively, for red, blue, green magenta and black). The solid curves are the results of the analytical calculations while the markers represent numerical ones. The dashed lines refer to the PIA gain. The signal and idler input powers are 0.1 mW.

5. Results and Discussion

The 18 coupled equations with the previously described linear and nonlinear terms have been solved through a Runge-Kutta algorithm. The nonlinear phase matching condition $\Phi = 0$ is assumed and both pumps have the same input power. A slight shift from the phase matching condition can be tolerated, as shown in [13].

For the PIA regime, the gain and the conversion efficiency numerically calculated are represented in Fig. 3(a) and (b) (black curves), respectively; the results of the analytical formulas (13) and (15) (red curves) are in an excellent agreement. It is also found that all other FWM processes are weakly contributing to the dynamic. The signal-idler frequency degeneracy implies that, in the PIA regime, it is possible to achieve an efficient mode conversion. However, the most intriguing results are to be found in the PSA regime. In Fig. 4, we compare the signal gain numerically calculated as a function of the phase ϕ_T, with the theoretical values given by (13), (16), and (17), for various values of input pump powers for the PSA regime. The value of the PIA gain is also represented as a constant reference in Fig. 4 as well.

Supported by the very good agreement between numerical and analytical results, we exploit the analytical formulas to predict features of the PSA regime that can find a valuable application in the context of mode processing. From (16) and (17) the maximum and minimum gains are found, respectively, for $\phi_T^{Max} = \arctan[-\Phi/(2g\coth(gL))]$ and $\phi_T^{min} = \phi_T^{MAX} + \pi$; both depend on the phase mismatch but not on the input amplitude unbalance R, generalizing to the present multimode case a result already known for single mode fibers [15]. Hereinafter, we assume perfect nonlinear phase matching ($\Phi = 0$), so two compact expressions for the maximum gain ($\phi_T^{MAX} = 0$) and for the

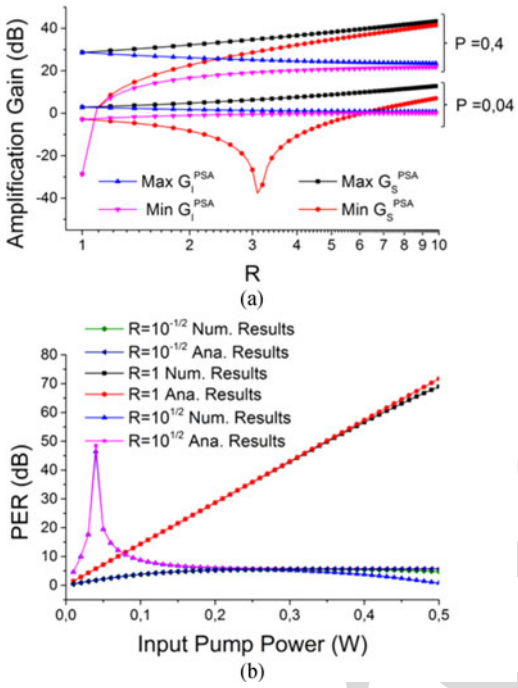

Fig. 5. (a) Black, red, blue, and magenta curves represent, respectively, G_S^{MAX}, G_S^{min}, G_I^{MAX}, and G_I^{min} as a function of R for two values of the input pump powers 0.04 W and 0.4 W. (b) Signal PER as a function of the input pump power for three values of the input amplitude disequilibrium $R = 1/\sqrt{10}, 1, \sqrt{10}$. The signal input power is 0.1 mW.

minimum gain ($\phi_T^{min} = \pi$) are found:

$$G_{S,I}^{MAX} = \left\{1 + \sinh^2\left(gL_{eff}\right)\left[1 + U_{S,I}^2 + 2U_{S,I}\coth\left(gL_{eff}\right)\right]\right\}\exp(-\alpha L) \quad (19)$$

$$G_{S,I}^{min} = \left\{1 + \sinh^2\left(gL_{eff}\right)\left[1 + U_{S,I}^2 - 2U_{S,I}\coth\left(gL_{eff}\right)\right]\right\}\exp(-\alpha L). \quad (20)$$

Note that the difference between the maximum and the minimum gain actually depends on two terms: $\coth\left(gL_{eff}\right)$, that is pump power dependent, and $U_{S,I}$ that depends only on the input signal/idler unbalance. Let us remark that the latter dependence is scarcely explored in the literature [27]. By inserting (19) and (20) into the PER definition [see (18)] and upon differentiation with respect to $U_{S,I}$ the condition maximizing the PER is simply given by $R_{MAX} = \coth\left(gL_{eff}\right)$ for the signal and $R_{MAX} = 1/\coth\left(gL_{eff}\right)$ for the idler. For high gain (i.e., under the condition $gL_{eff} > 3$) we have $\coth\left(gL_{eff}\right) \simeq 1$ an so the maximum signal PER is achieved for $R \simeq 1$. Note that high gain is the condition mainly exploited in previous studies of PSA in SMFs; in fact the results of [15, Fig. 4] are comparable to what we present in Fig. 5(a) for the FMF under the condition of large gain (set of curves for $P_{P1} = P_{P2} = 0.4$ W, $G_S^{MAX} \simeq 28$ dB). From Fig. 5(a), we can clearly observe that the maximum PER is achieved when G_S^{min} reaches a deep minimum. From the physical viewpoint this condition means that the signal and idler waves are actually depleted (signal and idler photons are annihilated to generate pump photons). If the condition $R = R_{MAX}$ was exactly satisfied, the minimum gain of (20) would go to zero and the PER [see. (18)] to infinity. From a practical viewpoint the weak differences in the input unbalance ratio, the imperfect nonlinear phase matching conditions and other fiber imperfections will lead to finite PER values. The dependence of the PER on the input pump powers is shown in Fig. 5(b) (once again with an excellent agreement between numerical calculations and theoretical result). For $R = 1$, the PER increases steadily with power until saturation occurs. In previous experiments in SMFs [15] the condition $R \simeq 1$ was used and therefore high pump

IEEE Proof

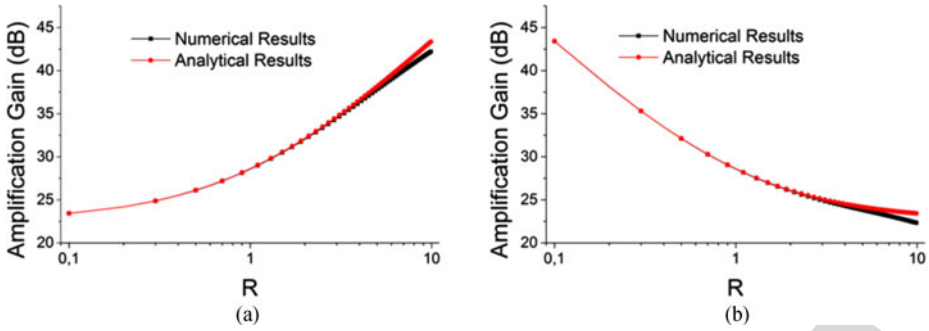

Fig. 6. (a) Maximum signal gain G_S^{MAX} and (b) maximum idler gain G_I^{MAX} as a function of R. The black curves are the results of the numerical calculations while the red curves of the analytical calculations. The input pump powers are 0.4 W (satisfying the condition $gL_{eff} > 3$), the input signal power is 0.01 mW, and $\Phi = 0$.

power was required to maximize the PER. Let us stress that the latter condition is subject to many possible impairments like pump depletion (also caused by Brillouin and Raman scattering) and gain saturation.

However, we highlight that if the aim is to realize mode processing, the condition of low pump powers ($gL_{eff} < 1$) can be also exploited. In this case the condition maximizing the PER yields $R_{MAX} = \coth(gL_{eff}) \neq 1$. This feature is confirmed in Fig. 5(a) by observing the set of curves for $P_{P1} = P_{P2} = 0.04$ W ($G_S^{MAX} \simeq 4$ dB): the maximum signal depletion (and PER) occurs for $R_{MAX} = \coth(gL_{eff}) \simeq 3.115$. Remarkably for this value of R the idler wave presents a negligible PER (about 2 dB). In fact to maximize the PER for the idler the condition $R_{MAX} = 1/\coth(gL_{eff}) \simeq 0.321$ must be imposed. In Fig. 5(b) the power dependence of the signal PER is presented also for $R = \sqrt{10}$ and $R = 1/\sqrt{10}$ (i.e. $\pm$ 10 dB input power disequilibrium). Note that the signal PER is maximized for a well defined, small value of the pump powers (low gain) for which the condition $R = \sqrt{10} \simeq R_{MAX} = \coth(gL_{eff})$ holds. Conversely, for the inverse value of R a negligible PER is found at all pump powers. The explanation of this behaviour are again the Manley-Rowe relations [23]. When $R > 1$ (input idler more powerful than input signal) the phase-sensitive depletion can be strong for the signal but still negligible for the idler (and vice versa for $R < 1$). This effect could find application to realize a modal filter providing a large (a few tens of decibels seem feasible) tunable phase-sensitive extinction ratio on one mode, while leaving the other mode essentially unaffected. This is also very attractive because of the low pump power requirements (few tens of mW). In the context of FWM processing of modes is also interesting to remark the consequences of Manley-Rowe relations when high gain ($gL_{eff} > 3$) is imposed. In fact, from Eqs. 19 when $\coth(gL_{eff}) \simeq 1$ the following is found in terms of the number of signal and idler photons

$$N_S(L) = G_S^{PSA} N_S(0) \simeq \left[1 + (1+R)^2 \sinh^2(gL_{eff})\right] \exp(-\alpha L) N_S(0) \tag{21}$$

$$N_I(L) = G_I^{PSA} N_I(0) \simeq \left[1 + \left(\frac{1+R}{R}\right)^2 \sinh^2(gL_{eff})\right] \exp(-\alpha L) N_I(0). \tag{22}$$

From (21) and (22) and recalling that $N_I(0) = R^2 N_S(0)$, it is straightforwardly found that the number of photons added to each wave amounts to

$$\Delta N = (1+R)^2 \sinh^2(gL_{eff}) \exp(-\alpha L) N_S(0). \tag{23}$$

Since $\Delta N \gg N_{S,I}(0)$, because $\sinh^2(gL_{eff}) \gg 1$, then the signal and idler output powers tends to become equal $N_{S,I}(L) \simeq \Delta N$ regardless the input power disequilibrium. This is confirmed in Fig. 6 where we present the gain for the signal (a) and for the idler (b) as a function of R. Once again the agreement between the analytical and the numerical values is excellent up to when the idler

IEEE Proof

power becomes large enough to induce pump depletion. Note that this feature can not be found in multimode fiber amplifiers based on doped fibers or Raman scattering [33], [34] where such Manley-Rowe relations do not hold. Finally, let us highlight two additional issues of all presented features: a) They are expected to be very fast; in fact, FWM is practically instantaneous and so modification of the output will mainly be set by the fiber propagation delays; b) they are general, i.e., apply also for PSA in SMFs.

6. Conclusion

We have considered a four-wave mixing process in a few mode fiber supporting two families of modes, for which the signal and the idler waves are frequency degenerate but propagate in non-degenerate modes. By neglecting the pump depletion and the mode coupling, we derived analytical expressions for the parametric gain and the conversion efficiency for both the phase-insensitive and the phase-sensitive amplification regimes. To test the analytical formulas we developed a full numerical model of the nonlinear interaction, that accounts for all possible nonlinear terms, for the pump depletion, for the losses and for the mode coupling due to residual birefringence and core ellipticity. The analytical findings are always in excellent agreement with the full numerical solutions for a few mode fiber characterized by a low mode coupling strength. Then, we highlighted a few interesting features associated to the phase sensitive four-wave mixing mode processing. In this regime, an extremely large phase-sensitive extinction ratio of one specific mode can be achieved, while keeping the other mode essentially unaffected, at low pump powers. This effect could be exploited for realizing a tunable modal filter. Finally, in the high gain regime we predict that such amplifier self-equalizes the output mode powers regardless their input power disequilibrium.

References

[1] D. J. Richardson, "Filling the light pipe," *Science*, vol. 30, pp. 327–328, 2010.
[2] D. J. Richardson, J. M. Fini, and L. E. Nelson, "Space-division multiplexing in optical fibres," *Nature Photon.*, vol. 7, pp. 354–362, 2013.
[3] G. Li and X. Liu, "Focus issue: Space multiplexed optical transmission," *Opt. Exp.*, vol. 19, pp. 16574–16575, 2011.
[4] C. Koebele, M. Salsi, G. Charlet, and S. Bigo, "Nonlinear effects in mode division multiplexed transmission over few-mode optical fiber," *IEEE Photon. Technol. Lett.*, vol. 23, pp. 1316–1318, 2011.
[5] A. Mecozzi, C. Antonelli, and M. Shtaif, "Nonlinear propagation in multi-mode fibers in the strong coupling regime," *Opt. Exp.*, vol. 20, pp. 11673–11678, 2012.
[6] A. Mecozzi, C. Antonelli, and M. Shtaif, "Coupled Manakov equations in multimode fibers with strongly coupled groups of modes," *Opt. Exp.*, vol. 20, pp. 23436–23441, 2012.
[7] S. Mumtaz, R.-J. Essiambre, and G. P. Agrawal, "Nonlinear propagation in multimode and multicore fibers: generalization of the Manakov equations," *J. Lightw. Technol.*, vol. 31, no. 3, pp. 398–406, Feb. 2013.
[8] R. H. Stolen and J. E. Bjorkholm, "Parametric amplification and frequency conversion in optical fibers," *IEEE J. Quantum Electron.*, vol. QE-18, no. 7, pp. 1062–1072, Jul. 1982.
[9] F. Poletti and P. Horak, "Description of ultrashort pulse propagation in multimode optical fibers," *J. Opt. Soc. Amer B*, vol. 25, pp. 1645–1654, 2008.
[10] F. Poletti and P. Horak, "Dynamics of femtosecond supercontinuum generation in multimode fibers," *Opt. Exp.*, vol. 17, pp. 6134–6147, 2009.
[11] A. Ben Salem, A. Trichili, R. Cherif, and M. Zghal, "Rigorous study of supercontinuum generation in few mode fibers," *Appl. Opt.*, vol. 16, pp. 4317–4322, 2016.
[12] R. J. Essiambre *et al.*, "Experimental investigation of inter-modal four-wave mixing in few-mode fibers," *IEEE Photon. Technol. Lett.*, vol. 25, no. 6, pp. 539–541, Mar. 2013.
[13] Y. Xiao *et al.*, "Theory of intermodal four-wave mixing with random linear mode coupling in few-mode fibers," *Opt. Exp.*, vol. 22, pp. 32039–32059, 2014.
[14] W. Pan, Q. Jin, X. Li, and S. Gao, "All-optical wavelength conversion for mode-division multiplexing signals using four-wave mixing in a dual-mode fiber," *J. Opt. Soc. Amer. B*, vol. 32, pp. 2417–2424, 2015.
[15] J. Kakande *et al.*, "Detailed characterization of a fiber-optic parametric amplifier in phase-sensitive and phase-insensitive operation," *Opt. Exp.*, vol. 18, pp. 4130–4137, 2010.
[16] M. E. Marhic, *Fiber Optical Parametric Amplifiers, Oscillators and Related Devices*. Cambridge, U.K.: Cambridge Univ. Press, 2007.
[17] Z. Tong *et al.*, "Towards ultrasensitive optical links enabled by low-noise phase-sensitive amplifiers," *Nature Photon.*, vol. 5, pp. 430–436, 2011.
[18] M. Annamalai and M. Vasilyev, "Phase-sensitive multimode parametric amplification in a parabolic-index waveguide," *IEEE Photon. Technol. Lett.*, vol. 24, no. 21, pp. 1949–1952, Nov. 2012.

IEEE PROOF

[19] C. J. McKinstrie and S. Radic, "Phase-sensitive amplification in a fiber," *Opt. Exp.*, vol. 12, pp. 4973–4979, 2004.
[20] G. P. Agrawal, *Nonlinear Fiber Optics*. New York, NY, USA: Academic, 2001, ch. 5, Eq. 5.1.9.
[21] M. Santagiustina, C. G. Someda, G. Vadalá, S. Combrié, and A. De Rossi, "Theory of slow light enhanced four-wave mixing in photonic crystal waveguides," *Opt. Exp.,* vol. 18, 2010, Art. no. 21024.
[22] S. Roy, M.Santagiustina, P. Colman, S. Combrié, and A. De Rossi, "Modeling the dispersion of the nonlinearity in slow mode photonic crystal waveguide," *IEEE Photon. J.*, vol. 4, no. 1, pp. 224–233, Feb. 2012.
[23] R. W. Boyd, "Wave-equation description of nonlinear optical interactions," in *Nonlinear Opt.*, New York, NY, USA: Academic, 1992, ch. 2.
[24] R. J. Essiambre, R. W. Tkach, and R. Ryf, "Fiber nonlinearity and capacity: Single-mode and multimode fibers," in Optical Fiber Telecommunications," vol. VI B, I. Kaminow, T. Li, and A. E. Willner, Eds. New York, NY, USA: Academic, 2013, ch. 1, pp. 1–37.
[25] S. Roy, M. Santagiustina, A. Willinger, G. Eisenstein, S. Combrié, and A. De Rossi, "Parametric gain and conversion efficiency in nanophotonic waveguides with dispersive propagation coefficients and loss," *J. Lightw. Technol.*, vol. 32, no. 6, pp. 1177–1182, Mar. 2014.
[26] R. Slavík *et al.*, "All-optical phase and amplitude regenerator for next-generation telecommunications systems," *Nature Photon.*, vol. 4, pp. 690–695, 2010.
[27] Z. Tong, C. Lundström, P. A. Andrekson, M. Karlsson, and A. Bogris, "Ultralow noise, broadband phase-sensitive optical amplifiers, and their applications," *IEEE J. Sel. Topics Quantum Electron.*, vol. 18, no. 2, pp. 1016–1032, Mar./Apr. 2012.
[28] M. A. Ettabib *et al.*, "All-optical phase regeneration with record PSA extinction ratio in a low-birefringence silicon germanium waveguide," *J. Lightw. Technol.* vol. 34, no. 17, pp. 3993–3998, Sep. 2016.
[29] D. Marcuse, *Theory of Dielectric Optical Waveguides*. New York, NY, USA: Academic, 1991.
[30] L. Palmieri, "Coupling mechanism in multimode fibers," *Proc. SPIE*, vol. 9009, 2013, Art. no. 90090G.
[31] L. Palmieri and A. Galtarossa, "Coupling effects among degenerate modes in multimode optical fibers," *IEEE Photon. J.*, vol. 6, no. 6, Dec. 2014, Art. no. 0600408.
[32] P. K. A. Wai and C. R. Menyuk, "Polarization mode dispersion, decorrelation, and diffusion in optical fibers with randomly varying birefringence," *J. Lightw. Technol.*, vol. 14, no. 2, pp. 148–157, Feb. 1996.
[33] S.-ul Alam, Y. Jung, Q. Kang, F. Poletti, J. K. Sahu, and D. J. Richardson, "Current status of few mode fiber amplifiers for spatial division multiplexed transmission," *J. Opt.*, pp. 1–10, 2015.
[34] R. Ryf, R.-J. Essiambre, J. von Hoyningen-Huene, and P. J. Winzer, "Analysis of mode-dependent gain in Raman amplified few-mode fiber," *in Proc. OFC*, 2012, Paper OW1D.2.

Q1

IEEE Proof

Queries

Q1. Author: Please provide volume in Ref. [33].

IEEE Proof